


# Gluon Wigner distributions under transverse polarization at non-zero skewness

Sujit Jana Kenil Solanki Vikash Kumar Ojha<sup>†</sup> 

Department of Physics, Sardar Vallabhbhai National Institute of Technology, Surat, 395 007, Gujarat, India

**Abstract:** We investigate the Wigner distributions of gluons at non-zero skewness using light-front wave functions within the dressed quark model, where the target state is a quark dressed with a gluon in the leading-order Fock space expansion. The analyses focus on the configurations wherein the gluon and/or the target are transversely polarized. Subsequently, we derive analytical expressions for the Wigner distributions in the boost-invariant longitudinal space ( $\sigma$ ) for transversely polarized configurations. Resultantly, a diffraction-like oscillatory pattern is yielded in  $\sigma$ -space, which is analogous to that reported previously for unpolarized and longitudinally polarized gluons.

**Keywords:** skewness, Wigner distributions

**DOI:** 10.1088/1674-1137/ae4325 **CSTR:** 32044.14.ChinesePhysicsC.50051001

## I. INTRODUCTION

A key objective of quantum chromodynamics (QCD) is the elucidation of the three-dimensional structure of hadrons through their underlying quark and gluon degrees of freedom [1, 2]. Among the most comprehensive hadronic tomography tools are Wigner distributions, which simultaneously encode the information of partons in position and momentum space, akin to phase-space distributions in quantum mechanics [3, 4]. Specifically, Wigner distributions are quasi-probability functions extensively employed in quantum optics, signal processing, and quantum field theory to analyze the phase-space structure and dynamics of quantum systems [5–7]. Although Wigner distributions are not directly observable owing to their quantum nature and lack of probabilistic interpretation, they are rich in structural information and provide insight into phenomena such as orbital angular momentum, spin–orbit correlations, and partonic correlations within nucleons [8–11].

In this context, numerous studies have investigated quark Wigner distributions, considering both zero and non-zero skewness scenarios [12–16]. By contrast, gluon Wigner distributions, particularly those involving polarization effects and skewed kinematics, remain relatively underexplored. Given the critical role of gluons in the momentum, spin, and small- $x$  dynamics of nucleons, gaining a deeper understanding of their phase-space distributions is essential. In this regard, elucidating the role

of gluons inside the proton, particularly their contributions to the proton spin through helicity and orbital angular momentum, is a primary objective of using the electron–ion collider (EIC), including the proposed EIC in China [1, 2]. Notably, some related recent studies have focused on gluon Wigner distributions [17–21]. Moreover, these gluon Wigner distributions are closely linked to generalized transverse momentum-dependent distributions (GTMDs), which unify and extend the framework of parton distribution functions (PDFs), transverse momentum-dependent distributions (TMDs), and generalized parton distributions (GPDs), thereby offering a broader perspective on the internal dynamics of hadrons [16, 22–25].

A particularly interesting scenario arises under the condition of non-zero skewness, wherein longitudinal momentum is transferred to the target. Specifically, a natural conjugate variable is introduced in coordinate space, giving rise to a new imaging dimension [26, 27]. In this context, a boost-invariant longitudinal coordinate, defined as  $\sigma = 1/2b^-P^+$ , plays a pivotal role. The variable,  $\sigma$ , is conjugate to the skewness parameter,  $\zeta$ , and allows for explorations of the gluon distribution spatial structure in the longitudinal direction in a frame-independent manner, whereby the phase-space interpretation of GTMDs and Wigner functions can be further substantiated.

This study investigates gluon Wigner distributions under non-zero skewness via the dressed quark model. The simple yet insightful framework thereof provides an

Received 30 September 2025; Accepted 6 February 2026; Accepted manuscript online 7 February 2026

<sup>†</sup> E-mail: vko@phy.svnit.ac.in



Content from this work may be used under the terms of the Creative Commons Attribution 3.0 licence. Any further distribution of this work must maintain attribution to the author(s) and the title of the work, journal citation and DOI. Article funded by SCOAP<sup>3</sup> and published under licence by Chinese Physical Society and the Institute of High Energy Physics of the Chinese Academy of Sciences and the Institute of Modern Physics of the Chinese Academy of Sciences and IOP Publishing Ltd

analytically tractable environment for investigating gluon dynamics. Specifically, transverse polarization configurations of the target and/or the gluon are analyzed, with notable distortions in the distributions ultimately observed. The results pertaining to the unpolarized and longitudinal polarization of gluons have been presented previously [28]. These polarization effects are critical for clarifying spin–momentum correlations and are relevant in the context of gluon orbital angular momentum and spin decomposition in nucleons.

Our analyses ultimately reveal a diffraction-like pattern of the gluon Wigner distributions in the  $\sigma$ -space for configurations involving a transversely polarized gluon and/or target. This behavior is qualitatively similar to that previously reported for unpolarized and longitudinally polarized configurations. Thus, our results indicate that the gluon Wigner distributions in the boost-invariant longitudinal space are sensitive to both the squared momentum transfer  $-t$  and polarization of the system.

The manuscript is organized as follows. Section II introduces the light-front conventions, outlines the relevant kinematic setup, and details the dressed quark model employed in our analysis. Section III defines the gluon Wigner distributions, focusing on the non-zero skewness regime, and Section III.A presents the analytical expressions for the gluon Wigner distributions in the boost-invariant longitudinal impact parameter space. Section IV details the numerical results and an account of the physical implications, and Section V provides the conclusions.

## II. DRESSED QUARK MODEL AND KINEMATICS

We herein employ the dressed quark model to investigate the gluon Wigner distributions. The dressed quark, modeled as a spin-1/2 state comprising a bare quark and a gluon in the leading-order light-front Fock space expansion, offers a simple yet insightful framework for analyzing gluon Wigner distributions. This model has been leveraged earlier to investigate the other relevant distribution functions, orbital angular momentum, and spin–orbit correlations of quarks and gluons [11, 12, 29–31].

We adopt the light-front coordinate system  $(x^+, x^-, x_\perp)$ , where  $x^+$  is the light-front time, and  $x^-$  is light-front longitudinal spatial coordinate, defined as  $x^\pm = x^0 \pm x^3$  [32]. The total squared momentum transfer to the target is given by  $t = \Delta^2 = (p - p')^2$  and the longitudinal momentum asymmetry between the initial and final target states is characterized by the skewness parameter,  $\xi$ , defined as

$$\xi = \frac{\Delta^+}{2P^+},$$

where  $P^+ = \frac{p^+ + p'^+}{2}$  is the average longitudinal mo-

mentum of the target. Under a symmetric frame [33], in which the average momentum is defined as  $P = 1/2(p + p')$ , the initial and final target states are parameterized as

$$p = \left( (1 + \xi)P^+, \frac{\Delta_\perp}{2}, \frac{m^2 + \Delta_\perp^2/4}{(1 + \xi)P^+} \right), \quad (1)$$

$$p' = \left( (1 - \xi)P^+, -\frac{\Delta_\perp}{2}, \frac{m^2 + \Delta_\perp^2/4}{(1 - \xi)P^+} \right). \quad (2)$$

The momentum transfer is then expressed as

$$\Delta = p - p' = \left( 2\xi P^+, \Delta_\perp, \frac{t + \Delta_\perp^2}{2\xi P^+} \right),$$

and the invariant momentum transfer squared is expressed as

$$t = -\frac{4\xi^2 m^2 + \Delta_\perp^2}{1 - \xi^2}.$$

The dressed quark state with spin  $\sigma$  and momentum  $p$  can be expanded in Fock space up to the two-particle sector, incorporating the quark-gluon configuration [30, 31]

$$\begin{aligned} |p^+, p_\perp, \sigma\rangle &= \Phi^\sigma(p) b_{\sigma'}^\dagger(p) |0\rangle + \sum_{\sigma_1 \sigma_2} \int [dp_1] \int [dp_2] \\ &\times \sqrt{16\pi^3 p^+} \delta^3(p - p_1 - p_2) \Phi_{\sigma_1 \sigma_2}^\sigma(p; p_1, p_2) \\ &\times b_{\sigma_1}^\dagger(p_1) a_{\sigma_2}^\dagger(p_2) |0\rangle. \end{aligned} \quad (3)$$

The state is expressed as a superposition of a single-quark state and a two-particle quark-gluon state, where the light-front wavefunctions (LFWFs) encapsulate the non-perturbative information. Here,  $[dp] = \frac{dp^+ d^2 p_\perp}{\sqrt{16\pi^3 p^+}}$ ,  $\Phi^\sigma(p)$  represents the single-particle wavefunction with momentum  $p$  and spin  $\sigma$ .  $\Phi_{\sigma_1 \sigma_2}^\sigma(p; p_1, p_2)$  represents the two-particle light-front wavefunction and can be expressed in a boost-invariant form using the relationship  $\Psi_{\sigma_1 \sigma_2}^\sigma(x, q_\perp) = \Phi_{\sigma_1 \sigma_2}^\sigma \sqrt{P^+}$ . The momentum variables  $(x_i, q_{i\perp})$  are the Jacobi momenta, defined as

$$p_i^+ = x_i p^+, \quad q_{i\perp} = k_{i\perp} + x_i p_\perp, \quad (4)$$

and they obey the following conditions:

$$\sum_i x_i = 1, \quad \sum_i q_{i\perp} = 0. \quad (5)$$

Assigning  $(x_1, q_{1\perp}) \equiv (x, q_\perp)$  to the quark, and  $(x_2, q_{2\perp}) \equiv$

$(x_g, q_{\perp g})$  to the gluon, we obtain

$$x + x_g = 1 \Rightarrow x_g = 1 - x, \quad (6)$$

$$\text{and } q_{\perp} + q_{\perp g} = 0 \Rightarrow q_{\perp g} = -q_{\perp}. \quad (7)$$

The longitudinal momentum fraction of the gluon with respect to the target is  $x_g = k_g^+/P^+$ , and the corresponding four-momentum of the gluon is

$$k_g \equiv (x_g P^+, k_{\perp g}, k_g^-). \quad (8)$$

### III. GLUON WIGNER DISTRIBUTION AT NON-ZERO SKEWNESS

We investigate the gluon Wigner distributions within the dressed quark model, focusing on non-zero skewness scenarios. These distributions are constructed using the LFWFs and defined via the Fourier transform of gluon-gluon correlators in longitudinal boost-invariant space. The general expression for the gluon Wigner distribution is given by [34, 21, 29]

$$\begin{aligned} xW_{\lambda\lambda'}(x, k_{\perp}, \Delta_{\perp}, \sigma) &= \int \frac{d\xi}{2\pi} e^{i\sigma\xi} \int \frac{dz^- d^2 z_{\perp}}{2(2\pi)^3 p^+} e^{ik \cdot z} \\ &\times \langle p^+, \frac{\Delta_{\perp}}{2}, \lambda' | \Gamma^{ij} F^{+i} \left(-\frac{z}{2}\right) \mathcal{W} F^{+j} \left(\frac{z}{2}\right) \mathcal{W}' | p^+, \frac{\Delta_{\perp}}{2}, \lambda \rangle_{z^+=0}. \end{aligned} \quad (9)$$

Here, the skewness parameter,  $\zeta$ , denotes the longitudinal momentum transfer to the target, and  $\sigma$  represents the longitudinal impact parameter space variable conjugate to  $\zeta$  [22]. The field strength tensors  $F^{+i}$  are evaluated at two spatially separated points and connected via Wilson lines  $\mathcal{W}$  and  $\mathcal{W}'$ , ensuring gauge invariance. The gauge-invariant Wilson line  $\mathcal{W}$  connecting two points  $z_1$  and  $z_2$  is defined as

$$\mathcal{W}(z_1, z_2) = \mathcal{P} \left[ \exp(-ig \int_{z_1}^{z_2} d\eta^\mu A_\mu(\eta)) \right].$$

The Wilson line  $\mathcal{W}(z_1, z_2)$  must be evaluated along some path connecting the point  $z_1$  and  $z_2$ . Here, we chose the path such that  $z^+ = 0$  as our fields are defined at  $z^+ = 0$ . Thus, we moved in the  $z^- - z_{\perp}$  plane. For connecting any two general point  $(z_1, z_2)$  in the  $z^- - z_{\perp}$  plane and representing a generic vector  $z^\mu = (z^+, z^-, z_{\perp})$ , we could define the longitudinal gauge link for point separated in the longitudinal direction, *i.e.*, if  $z_1 = (0, a^-, c_{\perp})$ ,  $z_2 = (0, b^-, c_{\perp})$  [35],

$$\mathcal{W}^-(a^-, b^-; c_{\perp}) = \mathcal{P} \left[ \exp(-ig \int_{a^-}^{b^-} d\eta^- A^+(0, \eta^-, c_{\perp})) \right],$$

and the transverse gauge link for transversely separated points, *i.e.*, if  $z_1 = (0, c^-, a_{\perp})$ ,  $z_2 = (0, c^-, b_{\perp})$ ,

$$\mathcal{W}^{\perp}(a_{\perp}, b_{\perp}; c^-) = \mathcal{P} \left[ \exp(ig \int_{a_{\perp}}^{b_{\perp}} d\eta_{\perp} A_{\perp}(0, c^-, \eta_{\perp})) \right].$$

Any two points in the  $z^- - z_{\perp}$  plane can be connected using the combination of the above-defined longitudinal and transverse gauge links. As we focus here on the bilocal operator  $F^{+i} \left(-\frac{z}{2}\right) \mathcal{W} F^{+j} \left(\frac{z}{2}\right)$ , we chose  $z_1 = -\frac{z}{2}$  and  $z_2 = \frac{z}{2}$ . We opted to connect these points by a staple-like path of straight lines passing through infinity. Thus, we have

$$\mathcal{W}\left(-\frac{z}{2}, \frac{z}{2}\right) \equiv \mathcal{W}\left(-\frac{z}{2}, \infty\right) \mathcal{W}\left(\infty, \frac{z}{2}\right)$$

$$\text{where, } \mathcal{W}\left(-\frac{z}{2}, \infty\right) = \mathcal{W}^-\left(-\frac{z^-}{2}, \infty^-; \frac{z_{\perp}}{2}\right) \mathcal{W}^{\perp}\left(-\frac{z_{\perp}}{2}, \infty_{\perp}; \infty^-\right)$$

$$\text{and, } \mathcal{W}\left(\infty, \frac{z}{2}\right) = \mathcal{W}^{\perp}\left(\infty_{\perp}, \frac{z_{\perp}}{2}; \infty^-\right) \mathcal{W}^-\left(\infty^-, \frac{z^-}{2}; \frac{z_{\perp}}{2}\right).$$

In the light-front gauge, we have  $A^+ = 0$ , whereby the longitudinal gauge link ( $\mathcal{W}^-$ ) becomes unity, and only the transverse gauge link remains:

$$\begin{aligned} \mathcal{W}\left(-\frac{z}{2}, \frac{z}{2}\right) &= \mathcal{W}^{\perp}\left(-\frac{z_{\perp}}{2}, \infty_{\perp}; \infty^-\right) \mathcal{W}^{\perp}\left(\infty_{\perp}, \frac{z_{\perp}}{2}; \infty^-\right) \\ &= 1 + ig \int_{-\frac{z_{\perp}}{2}}^{\frac{z_{\perp}}{2}} d\eta_{\perp} \cdot A_{\perp}(0, \infty^-, \eta_{\perp}) + \dots \end{aligned}$$

For our calculations, we retained only the leading-order term (unity), thereby neglecting all higher-order contributions. As we adopted the light-front gauge  $A^+ = 0$ , the field strength tensor simplifies to  $F^{+i} = \partial^+ A^i$ . The transverse components of the gauge field  $A^i$  are expressed in terms of creation and annihilation operators [31]

$$A^i\left(\frac{z}{2}\right) = \sum_{\lambda} \int \frac{dk^+ d^2 k_{\perp}}{2k^+(2\pi)^3} \left[ \epsilon_{\lambda}^i(k) a_{\lambda}(k) e^{-\frac{1}{2}k \cdot z} + \epsilon_{\lambda}^{*i}(k) a_{\lambda}^{\dagger}(k) e^{\frac{1}{2}k \cdot z} \right]. \quad (10)$$

At twist-two, the gluon Wigner distributions were constructed using the polarization projectors  $\Gamma^{ij} \in \{\delta_{\perp}^{ij}, -i\epsilon_{\perp}^{ij}, \Gamma^{RR}, \Gamma^{LL}\}$ , where  $R$  and  $L$  denote the right- and left-handed polarizations, respectively [24].

In the dressed quark model, the target state is expanded in terms of Fock components, and we retained only the quark-gluon two-particle sector. The two-particle LFWFs were obtained via the light-front Hamiltonian

perturbation theory, expressed as [31]

$$\Psi_{\sigma_1\sigma_2}^{\lambda a}(x, q_\perp) = \frac{g}{\sqrt{2(2\pi)^3}} T^a \chi_{\sigma_1}^\dagger O(x, q_\perp, m) \chi_\lambda(\epsilon_{\perp\sigma_2})^*, \quad (11)$$

where

$$O(x, q_\perp, m) = \frac{1}{\sqrt{1-x}} \left[ -2 \frac{q_\perp}{1-x} - \frac{(\sigma_\perp \cdot q_\perp) \sigma_\perp}{x} + im \sigma_\perp \frac{(1-x)}{x} \right]$$

denotes the spin-momentum structure, and

$$D(k_\perp, x) = m^2 - \frac{m^2 + k_\perp^2}{x} - \frac{k_\perp^2}{1-x}$$

is the energy denominator. The gluon-gluon correlators for different choices of  $\Gamma^{ij}$  were expressed, using the LFWFs, as overlaps of wave functions weighted by gluon polarization vectors. Here, the correlators depend on the kinematic variables,  $x_g = 1-x$ ; the skewness,  $\xi$ ; transverse momentum,  $k_{\perp g}$ ; and transverse momentum transfer to the target,  $\Delta_\perp$ . The polarization vectors  $\epsilon^L$  and  $\epsilon^R$  were constructed from the Cartesian components via  $\epsilon^{L(R)} = \epsilon^1 \mp i\epsilon^2$ .

The gluon-gluon correlator functions could be computed using the overlaps of two-particle LFWFs [21]. These correlators depend on the gluon polarization operator  $\Gamma^{ij}$  and polarization of the target state. Explicitly, the correlators are expressed as follows:

(a) For the unpolarized case, corresponding to  $\Gamma^{ij} = \delta_\perp^{ij}$ ,

$$W_{\sigma\sigma'}^{(\delta_\perp^{ij})} = - \sum_{\sigma_1, \lambda_1, \lambda_2} \Psi_{\sigma_1, \lambda_1}^{*\sigma'}(x'_g, q'_{\perp g}) \Psi_{\sigma_1, \lambda_2}^\sigma(y_g, q_{\perp g}) (\epsilon_{\lambda_2}^1 \epsilon_{\lambda_1}^{*1} + \epsilon_{\lambda_2}^2 \epsilon_{\lambda_1}^{*2}). \quad (12)$$

(b) For the longitudinally polarized case with  $\Gamma^{ij} = -i\epsilon_\perp^{ij}$ ,

$$W_{\sigma\sigma'}^{(-i\epsilon_\perp^{ij})} = -i \sum_{\sigma_1, \lambda_1, \lambda_2} \Psi_{\sigma_1, \lambda_1}^{*\sigma'}(x'_g, q'_{\perp g}) \Psi_{\sigma_1, \lambda_2}^\sigma(y_g, q_{\perp g}) (\epsilon_{\lambda_2}^1 \epsilon_{\lambda_1}^{*1} - \epsilon_{\lambda_2}^2 \epsilon_{\lambda_1}^{*2}). \quad (13)$$

(c) For the right-handed circular gluon polarization  $\Gamma^{ij} = \Gamma^{RR}$ ,

$$W_{\sigma\sigma'}^{(\Gamma^{RR})} = - \sum_{\sigma_1, \lambda_1, \lambda_2} \Psi_{\sigma_1, \lambda_1}^{*\sigma'}(x'_g, q'_{\perp g}) \Psi_{\sigma_1, \lambda_2}^\sigma(y_g, q_{\perp g}) \epsilon_{\lambda_2}^R \epsilon_{\lambda_1}^{*R}. \quad (14)$$

(d) For the left-handed circular gluon polarization  $\Gamma^{ij} = \Gamma^{LL}$ ,

$$W_{\sigma\sigma'}^{(\Gamma^{LL})} = - \sum_{\sigma_1, \lambda_1, \lambda_2} \Psi_{\sigma_1, \lambda_1}^{*\sigma'}(x'_g, q'_{\perp g}) \Psi_{\sigma_1, \lambda_2}^\sigma(y_g, q_{\perp g}) \epsilon_{\lambda_2}^L \epsilon_{\lambda_1}^{*L}. \quad (15)$$

Here, the kinematic variables are defined as follows:  $x_g = 1-x$  is the gluon longitudinal momentum fraction, where  $x'_g = x_g/(1-\xi)$ , and  $y_g = x_g/(1+\xi)$ . The initial and final gluon momenta are  $(y_g, q_{\perp g})$  and  $(x', q'_{\perp g})$ , respectively; the transverse momenta of the gluon in the initial and final states are expressed as

$$q_{\perp g} = -k_\perp + \frac{x_g \Delta_\perp}{2(1+\xi)}, \quad q'_{\perp g} = -k_\perp - \frac{x_g \Delta_\perp}{2(1-\xi)}, \quad (16)$$

and the circular polarization vectors of the gluon correspond to  $\epsilon_\lambda^{L(R)} = \epsilon_\lambda^1 \mp i\epsilon_\lambda^2$  [24].

The gluon Wigner distributions in boost-invariant longitudinal space were obtained by performing the Fourier transform of the correlators with respect to  $\xi$ :

$$\rho^\Gamma(x_g, \sigma, \Delta_\perp, k_\perp; S) = \int_0^{\xi_{\max}} \frac{d\xi}{2\pi} e^{i\sigma\xi} W^\Gamma(x_g, \xi, \Delta_\perp, k_\perp; S), \quad (17)$$

where  $S$  denotes the polarization of the target state, and  $\xi_{\max}$  is expressed as

$$\xi_{\max} = \frac{-t}{2m^2} \left( \sqrt{1 + \frac{4m^2}{-t}} - 1 \right), \quad \text{with } -t = \frac{4\xi^2 m^2 + \Delta_\perp^2}{1 - \xi^2}. \quad (18)$$

For an unpolarized gluon and target, the Wigner distribution is defined as

$$\rho_{UU}^g(x_g, \sigma, \Delta_\perp, k_\perp) = \frac{1}{2} \left[ \rho^{\delta_\perp^{ij}}(x, \sigma, \Delta_\perp, k_\perp; +\hat{e}_z) + \rho^{\delta_\perp^{ij}}(x, \sigma, \Delta_\perp, k_\perp; -\hat{e}_z) \right]. \quad (19)$$

By substituting the relevant expressions for the gluon-gluon correlator, we obtained an analytic form of the Wigner distribution as follows:

$$\rho_{UU}^g(x_g, \sigma, t, k_\perp) = \int_0^{\xi_{\max}} \frac{d\xi}{4\pi} e^{i\sigma\xi} \frac{\alpha_g}{x_g} \left[ -((4(1-\xi^2)k_\perp^2 - x_g^2 \Delta_\perp^2 + 4\xi x_g k_\perp \cdot \Delta_\perp)((1+x_g^2) + \xi(2-3\xi)) + 4m^2((1-x_g)^2 - \xi^2)^2) \right]. \quad (20)$$

The integrand includes kinematic and mass-dependent contributions along with the following factor:

$$\alpha_g = \frac{N \sqrt{1-\xi^2}}{D(q_{\perp g}, y_g) D^*(q'_{\perp g}, x'_g) x_g ((1-x_g)^2 - \xi^2)^{3/2}}. \quad (21)$$

Here,  $N = \frac{g^2 C_F}{2(2\pi)^3}$ , where  $g$  is the strong coupling constant, and  $C_F$  is the color factor.

### A. Transverse polarization case

The Wigner distributions for transversely polarized gluons, in conjunction with either an unpolarized or longitudinally polarized target, can be expressed in terms of helicity-dependent correlators [21]. For an unpolarized target, the gluon Wigner distributions with right- and left-handed transverse polarizations are defined as the helicity averages:

$$\rho_{UT}^{gR}(x_g, \sigma, \Delta_\perp, k_\perp) = \frac{1}{2} \left[ \rho^{\Gamma^{RR}}(x_g, \sigma, \Delta_\perp, k_\perp; +\hat{e}_z) + \rho^{\Gamma^{RR}}(x_g, \sigma, \Delta_\perp, k_\perp; -\hat{e}_z) \right], \quad (22)$$

$$\rho_{UT}^{gL}(x_g, \sigma, \Delta_\perp, k_\perp) = \frac{1}{2} \left[ \rho^{\Gamma^{LL}}(x_g, \sigma, \Delta_\perp, k_\perp; +\hat{e}_z) + \rho^{\Gamma^{LL}}(x_g, \sigma, \Delta_\perp, k_\perp; -\hat{e}_z) \right]. \quad (23)$$

For a longitudinally polarized target, the corresponding helicity-difference Wigner distributions are expressed as

$$\rho_{LT}^{gR}(x_g, \sigma, \Delta_\perp, k_\perp) = \frac{1}{2} \left[ \rho^{\Gamma^{RR}}(x_g, \sigma, \Delta_\perp, k_\perp; +\hat{e}_z) - \rho^{\Gamma^{RR}}(x_g, \sigma, \Delta_\perp, k_\perp; -\hat{e}_z) \right], \quad (24)$$

$$\rho_{LT}^{gL}(x_g, \sigma, \Delta_\perp, k_\perp) = \frac{1}{2} \left[ \rho^{\Gamma^{LL}}(x_g, \sigma, \Delta_\perp, k_\perp; +\hat{e}_z) - \rho^{\Gamma^{LL}}(x_g, \sigma, \Delta_\perp, k_\perp; -\hat{e}_z) \right]. \quad (25)$$

For a transversely polarized target, the gluon Wigner distributions depend on the polarization of the gluon and are defined as

$$\rho_{TT}^{g(R)i}(x_g, \sigma, \Delta_\perp, k_\perp) = \frac{1}{2} \left[ \rho^{\Gamma^{RR}}(x_g, \sigma, \Delta_\perp, k_\perp; +\hat{e}_i) + \rho^{\Gamma^{RR}}(x_g, \sigma, \Delta_\perp, k_\perp; -\hat{e}_i) \right], \quad (26)$$

$$\rho_{TT}^{g(L)i}(x_g, \sigma, \Delta_\perp, k_\perp) = \frac{1}{2} \left[ \rho^{\Gamma^{LL}}(x_g, \sigma, \Delta_\perp, k_\perp; +\hat{e}_i) + \rho^{\Gamma^{LL}}(x_g, \sigma, \Delta_\perp, k_\perp; -\hat{e}_i) \right], \quad (27)$$

$$\rho_{TU}^{gi}(x_g, \sigma, \Delta_\perp, k_\perp) = \frac{1}{2} \left[ \rho^{\delta_{ij}}(x_g, \sigma, \Delta_\perp, k_\perp; +\hat{e}_i) + \rho^{\delta_{ij}}(x_g, \sigma, \Delta_\perp, k_\perp; -\hat{e}_i) \right], \quad (28)$$

$$\rho_{TL}^{gi}(x_g, \sigma, \Delta_\perp, k_\perp) = \frac{1}{2} \left[ \rho^{-i\hat{e}_\perp}(x_g, \sigma, \Delta_\perp, k_\perp; +\hat{e}_i) + \rho^{-i\hat{e}_\perp}(x_g, \sigma, \Delta_\perp, k_\perp; -\hat{e}_i) \right]. \quad (29)$$

Here,  $\hat{e}_i$  denotes the transverse spin direction of the target, where  $i = x, y$ . The transverse polarization states are defined in terms of helicity eigenstates. For example,

$$|\pm \hat{e}_x\rangle = \frac{1}{\sqrt{2}} \left( \left| \frac{1}{2} \right\rangle \pm \left| -\frac{1}{2} \right\rangle \right).$$

The analytic expressions for the gluon Wigner distributions in the boost-invariant longitudinal position space ( $\sigma$ ) corresponding to various gluon and target polarization combinations were derived using two-particle light-front wave functions. The corresponding results for the transverse polarization configurations are presented in Eqs. (30)–(37), including the cases of transversely polarized gluons with unpolarized and longitudinally polarized targets, as well as transversely polarized targets. The integrals involve the skewness parameter,  $\xi$ , and the resulting Wigner distributions depend on the set of kinematic variables  $(x_g, \xi, k_\perp^2, \Delta_\perp^2, k_\perp \cdot \Delta_\perp)$ . Using the relationship in Eq. (18), we re-expressed the dependence on the transverse momentum transfer  $\Delta_\perp$  in terms of the Mandelstam variable,  $t$ , prior to performing the Fourier transform to the  $\sigma$ -space. The analytical expressions for  $\rho_{UU}^g$ ,  $\rho_{TU}^{gx}$ , and  $\rho_{TL}^{gx}$  in the dressed quark model are provided in Ref. [21] for zero skewness. Those for  $\rho_{UU}^g$ ,  $\rho_{TU}^{gx}$ , and  $\rho_{TL}^{gx}$  for non-zero skewness are given in Eqs. (20), (36), and (37), with the results of [21] being reproduced for the limit  $\xi \rightarrow 0$ .

$$\rho_{UT}^{gR}(x_g, \sigma, t, k_\perp) = \int_0^{\xi_{\max}} \frac{d\xi}{4\pi} e^{i\sigma\xi} \frac{\alpha_g}{x_g} \left[ -4m^2((1-x_g)^2 - \xi^2)^2 + (x_g^2 + 1 - \xi^2)(-4(1-\xi^2)k_\perp^2 + x_g^2 \Delta_\perp^2 - 4x_g \xi k_\perp \cdot \Delta_\perp - i(k_1 \Delta_2 - k_2 \Delta_1)) \right], \quad (30)$$

$$\rho_{UT}^{gL}(x_g, \sigma, t, k_\perp) = \int_0^{\xi_{\max}} \frac{d\xi}{4\pi} e^{i\sigma\xi} \frac{\alpha_g}{x_g} \left[ -4m^2((1-x_g)^2 - \xi^2)^2 - (1+x_g^2 - \xi^2)(4(1-\xi^2)k_\perp^2 - x_g^2 \Delta_\perp^2 + 4x_g \xi k_\perp \cdot \Delta_\perp + 4ix_g(k_1 \Delta_2 - k_2 \Delta_1)) \right], \quad (31)$$

$$\rho_{LT}^{gR}(x_g, \sigma, t, k_\perp) = \int_0^{\xi_{\max}} \frac{d\xi}{4\pi} e^{i\sigma\xi} \frac{\alpha_g}{x_g} \left[ 4m^2((1-x_g)^2 - \xi^2)^2 + (x_g^2 - 1 + \xi^2)(-4(1-\xi^2)k_\perp^2 + x_g^2 \Delta_\perp^2 - 4x_g \xi k_\perp \cdot \Delta_\perp - i(k_1 \Delta_2 - k_2 \Delta_1)) \right], \quad (32)$$

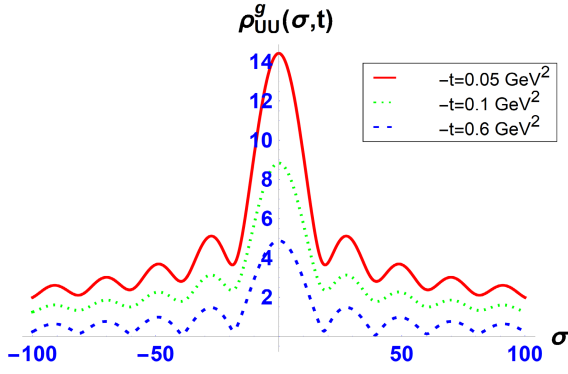


**Fig. 1.** (color online) First moment of the gluon Wigner distribution  $\rho_{UU}^g$  for various values of  $-t$ , corresponding to the unpolarized gluon in an unpolarized target.

$$\rho_{LT}^{gL}(x_g, \sigma, t, k_{\perp}) = \int_0^{\xi_{\max}} \frac{d\xi}{4\pi} e^{i\sigma\xi} \frac{\alpha_g}{x_g} \left[ -4m^2((1-x_g)^2 - \xi^2)^2 - (1-x_g^2 + \xi^2)(4(1-\xi^2)k_{\perp}^2 - x_g^2\Delta_{\perp}^2 + 4x_g\xi k_{\perp} \cdot \Delta_{\perp} + 4ix_g(k_1\Delta_2 - k_2\Delta_1)) \right], \quad (33)$$

$$\rho_{TT}^{g(R)x}(x_g, \sigma, t, k_{\perp}) = \int_0^{\xi_{\max}} \frac{d\xi}{4\pi} e^{i\sigma\xi} \alpha_g \left[ 4im(((1-x_g)^2 + \xi^2)(2\xi k_1 + 2ik_2 - x_g\Delta_1) - 2(1-x_g)\xi(2k_1 + 2i\xi k_2 - ix_g\Delta_2)) \right], \quad (34)$$

$$\rho_{TT}^{g(L)x}(x_g, \sigma, t, k_{\perp}) = \int_0^{\xi_{\max}} \frac{d\xi}{4\pi} e^{i\sigma\xi} \alpha_g \left[ 4m(((1-x_g)^2 + \xi^2)(2(i\xi k_1 + k_2) - ix_g\Delta_1) - 2(1-x_g)\xi(2(ik_1 + \xi k_2) - x_g\Delta_2)) \right], \quad (35)$$

$$\rho_{TU}^{gx}(x_g, \sigma, t, k_{\perp}) = \int_0^{\xi_{\max}} \frac{d\xi}{4\pi} e^{i\sigma\xi} \alpha_g \left[ 4im(2\xi(x_g^2 - 1 + \xi^2)k_1 - x_g((1-x_g)^2 + \xi^2)\Delta_1) \right], \quad (36)$$

$$\rho_{TL}^{gx}(x_g, \sigma, t, k_{\perp}) = \int_0^{\xi_{\max}} \frac{d\xi}{4\pi} e^{i\sigma\xi} \alpha_g \left[ 8m(((1-x_g)^2 + \xi^2) - 2(1-x_g)\xi^2)k_2 + (1-x_g)x_g\xi\Delta_2 \right]. \quad (37)$$

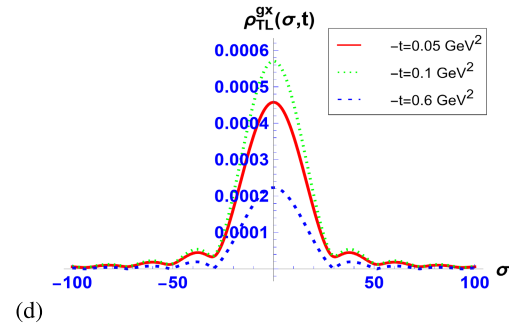
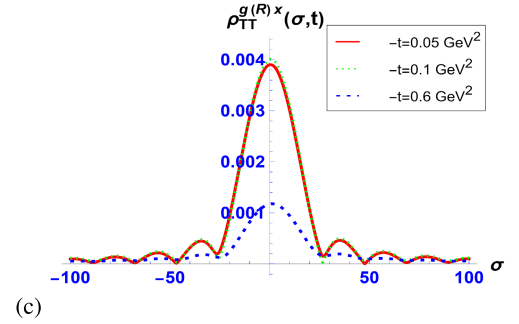
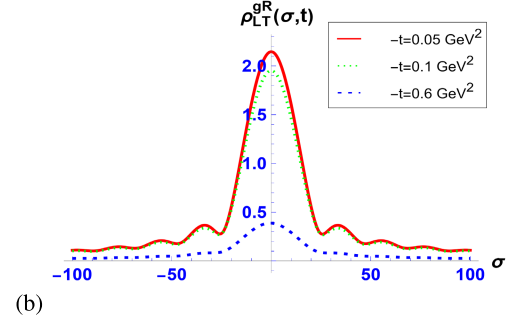
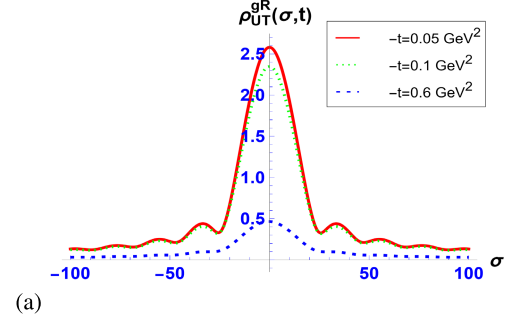


**Fig. 2.** (color online) First moment of the gluon Wigner distribution for a) transversely polarized gluon in unpolarized target  $\rho_{UT}^{gR}$ , b) transversely polarized gluon in longitudinally polarized target  $\rho_{LT}^{gR}$ , c) transversely polarized gluon and target  $\rho_{TT}^{g(R)x}$ , and d) longitudinally polarized gluon and transversely polarized target  $\rho_{TL}^{gx}$ .

#### IV. NUMERICAL ANALYSES AND DISCUSSION

The Wigner distributions were plotted for three different values of the squared momentum transfer,  $-t = 0.05$ ,

0.1, and 0.6 GeV<sup>2</sup>, for analyzing the impact of  $-t$  on the transversely polarized gluon Wigner distributions in  $\sigma$ -space. For all cases, the transverse momentum transfer,  $\Delta_{\perp}$ , was chosen to be perpendicular to the gluon transverse momentum,  $k_{\perp}$ , such that contributions from terms proportional to  $k_{\perp} \cdot \Delta_{\perp}$  could be suppressed. The mass of the dressed quark was fixed at 0.0033 GeV. Figure 1 displays the Wigner distribution for an unpolarized gluon in an unpolarized target, in the longitudinal impact parameter space. Figure 2 shows the Wigner distributions in  $\sigma$ -space for cases where the gluon and/or the target are transversely polarized. For all the plots of Figs. 1 and 2, the gluon longitudinal momentum fraction was fixed at  $x_g = 0.7$  and the transverse momentum at  $k_{\perp} = 0.2\hat{x}$  GeV. Figure 2 illustrates the distortions in the gluon Wigner distributions induced by the transverse polarization of the gluon and target state. Figs. 2(a) and 2(b) show the modification of the distribution when the gluon was transversely polarized in an unpolarized and longitudinally polarized target, and Figs. 2(c) and 2(d) show the plots when the target itself was transversely polarized. The magnitude of the gluon Wigner distributions was significantly reduced when the target was transversely polarized, relative to that in the cases of longitudinal polarization or an unpolarized target. For the distributions  $\rho_{UT}$  and  $\rho_{LT}$ , the peak magnitude increased monotonically as  $-t$  decreased. However, for  $\rho_{TT}$  and  $\rho_{TL}$ , the peak height exhibited a non-monotonic dependence on  $-t$ , peaking at  $-t = 0.1$  GeV<sup>2</sup> among the three chosen values of  $-t$ . A common occurrence across all the distributions was the emergence of a diffraction-like pattern in  $\sigma$ -space. These results indicate that such diffraction-like patterns persist in the longitudinal impact parameter space even in the case of transverse polarization of either the gluon or tar-

get, with the peak of the distribution exhibiting sensitivity to the magnitude of  $-t$ . Similar diffraction patterns have also been reported in earlier studies for gluons in cases involving unpolarized and longitudinally polarized gluons and targets within the same model [28].

## V. CONCLUSION

We investigated gluon Wigner distributions under transverse polarization using the dressed quark model for non-zero skewness scenarios within the light-front Hamiltonian formalism. Accordingly, the two-particle LFWFs were used to evaluate the gluon-gluon correlators for different transverse polarization configurations, and the associated Wigner distributions were derived in the longitudinal boost-invariant impact parameter space ( $\sigma$ ). Analytical expressions for the gluon Wigner distributions were obtained for cases wherein the gluon and/or the target were transversely polarized, and the gluon Wigner distributions  $\rho_{UU}^g$ ,  $\rho_{UT}^{gR}$ ,  $\rho_{LT}^{gR}$ ,  $\rho_{TT}^{g(R)x}$ , and  $\rho_{TL}^{gx}$  were analyzed in  $\sigma$ -space via the two-dimensional plots shown in Figs. 1 and 2. Overall, all distributions exhibited diffraction-like oscillatory behavior and sensitivity to the momentum transfer,  $-t$ , which is consistent with earlier findings for gluon Wigner distributions in unpolarized and longitudinally polarized configurations [28]. Similar oscillatory diffraction patterns have also been observed in studies on quark Wigner distributions within the dressed quark model and the light-front quark-diquark model [12, 22]. Although quark Wigner distributions under transverse polarization have been explored in various models, this study provides the first known analysis of gluon Wigner distributions under transverse polarization in the boost-invariant longitudinal impact parameter space.

## References

- [1] A. Accardi, J. L. Albacete, M. Anselmino *et al.*, *Eur. Phys. J. A* **52**(9), 268 (2016), arXiv: 1212.1701
- [2] D. P. Anderle, V. Bertone, X. Cao *et al.*, *Front. Phys.* **15**, 64701 (2021)
- [3] X. d. Ji, *Phys. Rev. Lett.* **91**, 062001. (2003), arXiv: hep-ph/0304037
- [4] A. V. Belitsky, X. d. Ji, and F. Yuan, *Phys. Rev. D* **69**, 074014 (2004), arXiv: hep-ph/0307383
- [5] M. Bastiaans, *JOSA* **69**(12), 1710 (1979)
- [6] G. W. Forbes, V. Man'ko, H. M. Ozaktas *et al.*, *JOSA A* **17**(12), 2274 (2000)
- [7] R. Radhakrishnan and V. K. Ojha, *Mod. Phys. Lett. A* **37**(37n38), 2250236 (2022)
- [8] C. Lorce and B. Pasquini, *Phys. Rev. D* **84**(1), 014015 (2011)
- [9] D. Chakrabarti, T. Maji, C. Mondal *et al.*, *Eur. Phys. J. C* **76**(7), 409 (2016), arXiv: 1601.03217
- [10] C. Lorce, B. Pasquini, X. Xiong *et al.*, *Phys. Rev. D* **85**, 114006 (2012), arXiv: 1111.4827
- [11] A. Mukherjee, S. Nair, and V. K. Ojha, *Phys. Rev. D* **90**(1), 014024 (2014)
- [12] V. K. Ojha, S. Jana, and T. Maji, *Phys. Rev. D* **107**(7), 074040 (2023)
- [13] X. Luan and Z. Lu, *Phys. Rev. D* **109**(9), 094016 (2024), arXiv: 2401.15596
- [14] W. Broniowski and E. Ruiz Arriola, *Acta Phys. Polon. B* **54**(7), 7 (2023), arXiv: 2307.14167
- [15] Y. Han, T. Liu, and B. Q. Ma, *Phys. Lett. B* **930**, 137127 (2022), arXiv: 2202.10359
- [16] Y. Yang, T. Liu, and B. Q. Ma, *Eur. Phys. J. C* **85**(5), 504 (2025), arXiv: 2505.06615
- [17] C. Tan and Z. Lu, *Eur. Phys. J. C* **85**(3), 355 (2025), arXiv: 2312.07997
- [18] R. Pasechnik and M. Taševský, *Phys. Rept.* (2024), 3 (1084), arXiv: 2310.10793
- [19] Y. Hagiwara, Y. Hatta, R. Pasechnik *et al.*, *Phys. Rev. D* **96**(3), 034009 (2017), arXiv: 1706.01765
- [20] R. Boussarie, Y. Hatta, B. W. Xiao *et al.*, *Phys. Rev. D* **98**(7), 074015 (2018), arXiv: 1807.08697
- [21] J. More, A. Mukherjee, and S. Nair, *Eur. Phys. J. C* **78**, 1

- (2018)
- [22] T. Maji, C. Mondal, and D. Kang, *Phys. Rev. D* **105**(7), 074024 (2022)
- [23] S. Meißner, K. Goeke, A. Metz *et al.*, *JHEP* **2008**(08), 038 (2008)
- [24] C. Lorce and B. Pasquini, *JHEP* **2013**(9), 1 (2013)
- [25] S. Kaur and H. Dahiya, *Nucl. Phys. B* **937**, 272 (2018)
- [26] S. Brodsky, D. Chakrabarti, A. Harindranath *et al.*, *Phys. Lett. B* **641**(6), 440 (2006)
- [27] S. J. Brodsky, D. Chakrabarti, A. Harindranath *et al.*, *Phys. Rev. D* **75**, 014003 (2007), arXiv: hep-ph/0611159
- [28] S. Jana, V. K. Ojha, and T. Maji, *Nucl. Phys. A* **1053**, 122958 (2024)
- [29] A. Mukherjee, S. Nair, and V. K. Ojha, *Phys. Rev. D* **91**(5), 054018 (2015)
- [30] A. Harindranath, R. Kundu, and W. M. Zhang, *Phys. Rev. D* **59**(9), 094012 (1999)
- [31] A. Harindranath and R. Kundu, *Phys. Rev. D* **59**(11), 116013 (1999)
- [32] A. Harindranath, (1996), arXiv: hep-ph/9612244
- [33] S. J. Brodsky, M. Diehl, and D. S. Hwang, *Nucl. Phys. B* **596**(1-2), 99 (2001)
- [34] X. Ji, X. Xiong, and F. Yuan, *Phys. Rev. D* **88**(1), 014041 (2013)
- [35] A. Bacchetta, L. Mantovani, and B. Pasquini, *Phys. Rev. D* **93**(1), 013005 (2016)